Electronic Supplementary Material (ESI) for Dalton Transactions.

SUPPORTING INFORMATION

Supplementary Material

Mechanistic Insight into Novel Sulfoxide Containing SABRE Polarisation Transfer Catalysts

Ben. J. Tickner[a] Jennifer S. Lewis[a], Richard O. John,[a] Adrian C. Whitwood[b] and Simon B. Duckett[a*]

[a]Centre for Hyperpolarisation in Magnetic Resonance (CHyM), University of York, Heslington, York, YO10 5NY, UK.

[b]Department of Chemistry, University of York, Heslington, York, YO10 5DD, UK.

*Corresponding author. E-mail: simon.duckett@york.ac.uk

Table of Contents

S1. Characterization of products

S1.1: NMR characterization data of 1

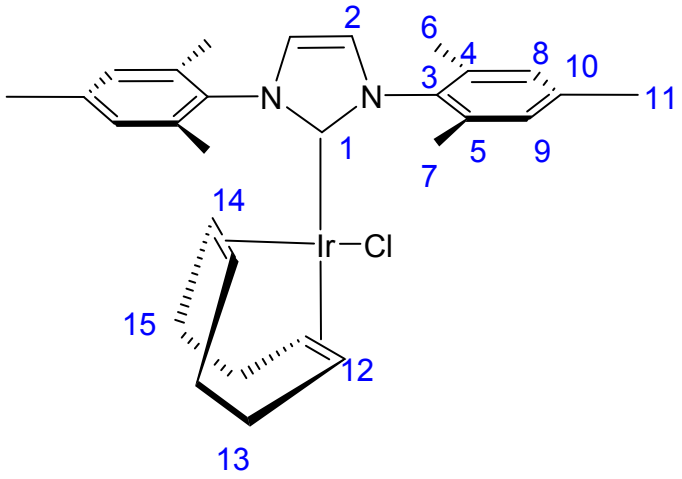

Figure S1: Structure of [IrCl(COD)(IMes)] (1) where the labels refer to the resonance numbers of Table S1.

Table S1: NMR characterisation data of [IrCl(COD)(IMes)] of Figure S1 in methanol-d_4 at 245 K.

Resonance	^{1}H	^{13}C
1	-	N/A
2	7.31	123.93
3	-	139.91
4	-	138.67
5	-	137.30
6	2.30	18.46
7	2.21	17.31
8	7.05	128.89
9	7.08	127.97
10	-	136.05
11	2.38	19.87
12	3.10	131.87
13	1.27, 1.64	28.52/33.04
14	3.99	121.16
15	1.38, 1.74	28.52/33.04

S1.2: NMR characterization data of 2

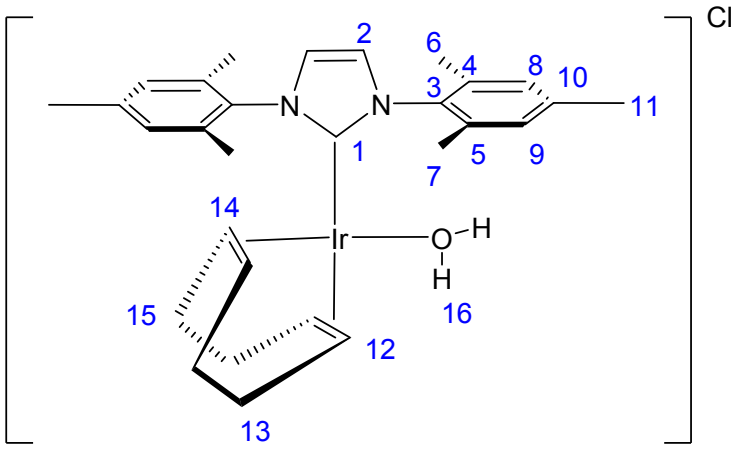

Figure S2: Structure of [Ir(COD)(IMes)(OH_2)]Cl (2) where the labels refer to the resonance numbers of Table S2.

Table S2: NMR characterisation data of [Ir(COD)(IMes)(OH_2)]Cl (2) of Figure S2 in methanol-d_4 at 245 K.

Resonance	^{1}H	^{13}C
1	-	N/A
2	6.96	122.48
3	-	139.77
4	-	N/A
5	-	N/A
6	2.17	19.25
7	2.16	16.64
8	6.72	128.34
9	6.72	128.71
10	-	N/A
11	2.30	17.28
12	3.01	N/A
13	1-2 ppm (overlap)	N/A
14	4.22	N/A
15	1-2 ppm (overlap)	N/A
16	8.15	-

S1.3: NMR characterization of 6

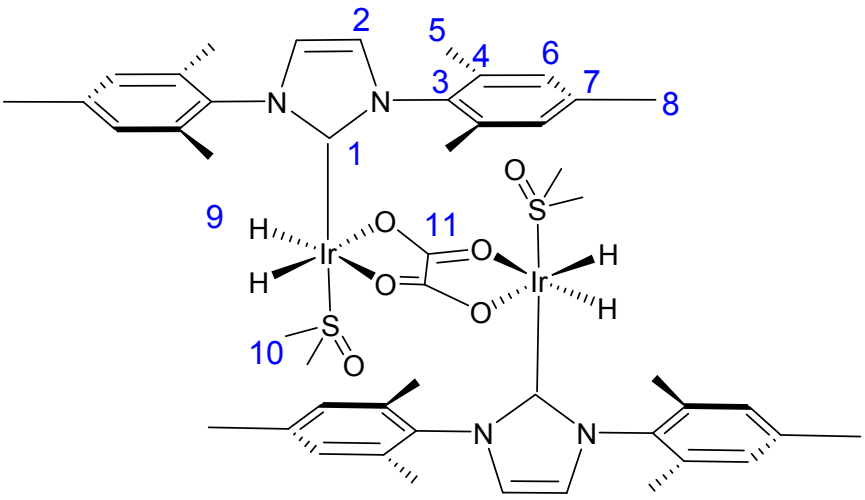

Figure S3: Structure of $[Ir_2(H)_4(IMes)_2(DMSO)_2(\eta^2\text{-}\kappa^2\text{-Oxalate})]$, 6 where the labels refer to the resonance numbers of Table S3.

Table S3: NMR characterisation data of $[Ir_2(H)_4(IMes)_2(DMSO)_2(\eta^2\text{-}\kappa^2\text{-Oxalate})]$, 6 of Figure S3 in methanol-d_4 at 245 K.

Resonance	^{1}H	^{13}C
1	-	~ 150-155
2	7.15	122.63
3	-	135.25
4	-	137.04
5	2.10	17.17
6	6.99	128.52
7	-	137.94
8	2.34	17.92
9	− 27.09	-
10	2.92	47.04
11	-	168.15

S1.4: X-ray diffraction of 5

Crystals were prepared by removing the H_2 atmosphere from a sample of [IrCl(COD)(IMes)] (2 mg), DMSO (1 µL), and sodium oxalate (2 mg) in 0.6 mL methanol and 50 µL H_2O and then layering ~3 mL degassed hexane slowly on top of the solution in the NMR tube and leaving it under N_2 for period of several days. A suitable crystal was selected and mounted on an Oxford Diffraction SuperNova- X-ray diffractometer. The crystal was kept at 110 K during data collection. Diffractometer control, data collection, initial unit cell determination, frame integration and unit-cell refinement was carried out with "CrysAlisPro".[1] Face-indexed absorption corrections were applied using spherical harmonics, implemented in SCALE3 ABSPACK scaling algorithm. Using Olex2,[2] the structure was solved with the ShelXT[3] structure solution program using Intrinsic Phasing and refined with the ShelXL[4] refinement package using Least Squares minimisation.
The hydrides were located by difference map with one of the Ir-H bond lengths subsequently restrained to be 1.6 angstroms.
The dichloromethane of crystallisation was disordered and modelled in two positions with refined occupancies of 0.771:0.229(3). The ADP of pairs of disordered atoms were constrained to be equal (C25 & C25a, Cl1 & Cl1a, Cl2 & Cl2a). The C-Cl bond lengths were restrained to be equal.
The occupancy of the partial water of crystallisation refined to 0.634(13).

Table S4. Crystal data and structure refinement.

Compound	**6**
Empirical formula	$C_{50}H_{70.54}Cl_4Ir_2N_4O_{7.27}S_2$
Formula weight	1434.28
Temperature/K	110.00(10)
Crystal system	triclinic
Space group	P-1
a/Å	9.7187(5)
b/Å	12.0086(7)
c/Å	13.3295(11)
α/°	85.912(6)
β/°	69.210(6)
γ/°	76.361(5)
Volume/Å^3	1413.21(17)
Z	1
ρ_{calc}g/cm^3	1.685
μ/mm^{-1}	11.827
F(000)	710.7
Crystal size/mm^3	0.163 × 0.052 × 0.018
Radiation	CuKα (λ = 1.54184)
2Θ range for data collection/°	7.094 to 134.126
Index ranges	-11 ≤ h ≤ 11, -9 ≤ k ≤ 14, -15 ≤ l ≤ 15
Reflections collected	9141
Independent reflections	5051 [R_{int} = 0.0319, R_{sigma} = 0.0472]
Data/restraints/parameters	5051/7/346
Goodness-of-fit on F^2	1.019
Final R indexes [I>=2σ (I)]	R_1 = 0.0303, wR_2 = 0.0730
Final R indexes [all data]	R_1 = 0.0354, wR_2 = 0.0768
Largest diff. peak/hole / e Å^{-3}	1.51/-1.45

S2. Density Functional Theory (DFT) Calculations

All DFT calculations were performed on the full molecule (without simplification) using the Gaussian 09 software package.[5] All structures were optimized in combination with solvent effects modelled with the integral equation formalism variant of the Polarizable Continuum Model (IEFPCM).[6-8] All calculations had the solvent specified as methanol. All calculations used the PBE0 DFT functional[9] and the basis set family defined as def2-SVP from Ahlrichs[10, 11] for all atoms (taken from the EMSL website)[12, 13] except hydride atoms and iridium. The hydride atoms were assigned the larger def2-TZVPP basis set[10, 11] and iridium was assigned the LANL08(f) basis set with the associated effective core potential (ECP).[14] Frequency calculations were used to confirm that the structures obtained were local minima along with zero-point energies and thermal corrections to the energy at 298.15 K. Single point calculations (again with solvation) were then undertaken with all atoms apart from Iridium assigned the larger basis sets from the def2-TZVPP family (the LANL08(f) basis set was maintained for iridium). The thermal energy corrections were then applied to obtain chemical enthalpies and free energies.[16] This approach has previously been used to model the reactions of similar systems.[17, 18] The calculations were checked for Basis Set Superposition Errors (BSSE). The resulting counterpoise calculation revealed that errors of around 5 kJ mol^{-1} were present in all systems and so corrections were applied appropriately.[19, 20] Additional calculations were performed which included the GD3BJ empirical dispersion correction from Grimme which includes Beck-Johnson dampling.[15] These additional calculations are not quoted in this work and were not used as doing so yielded relative energies that are inconsistent with experimental observations.

It should be noted that the equilirium free energies presented in Tables 1, 2 and 4 are relative to a zero point which includes all of the species in the individual table. For example, for Table 1 this would be the complex, DMSO, H_2O and CH_3OH in a equimolar amount.

Table S5: Relative enthalpy (H) and Gibbs free energies (G) of H_2 addition products to 1 and 2 according to DFT calculations. These energies are relative to those of 1 or 2 respectively and do not reflect transition state barriers.

Complex	Axis of H_2 addition	H /kJ mol^{-1}	G /kJ mol^{-1}
1	COD-Ir-X	-32.9	4.7
1	COD-Ir-IMes	16.9	57.0
2	COD-Ir-X	-55.2	-15.1
2	COD-Ir-IMes	11.2	57.8

S3. Isolation of 3

NMR characterization data for **3** has been previously reported.[21]
HR-ESI$^+$/MS (m/z): for **3** $[C_{25}H_{38}ClIrN_2O_2S_2 - C_2H_8ClOS]^+$, calcd 575.1703, found 575.1712.

Solutions of **3** in methanol-d_4 are unstable when exposed to oxygen although **3** can be isolated as a solid

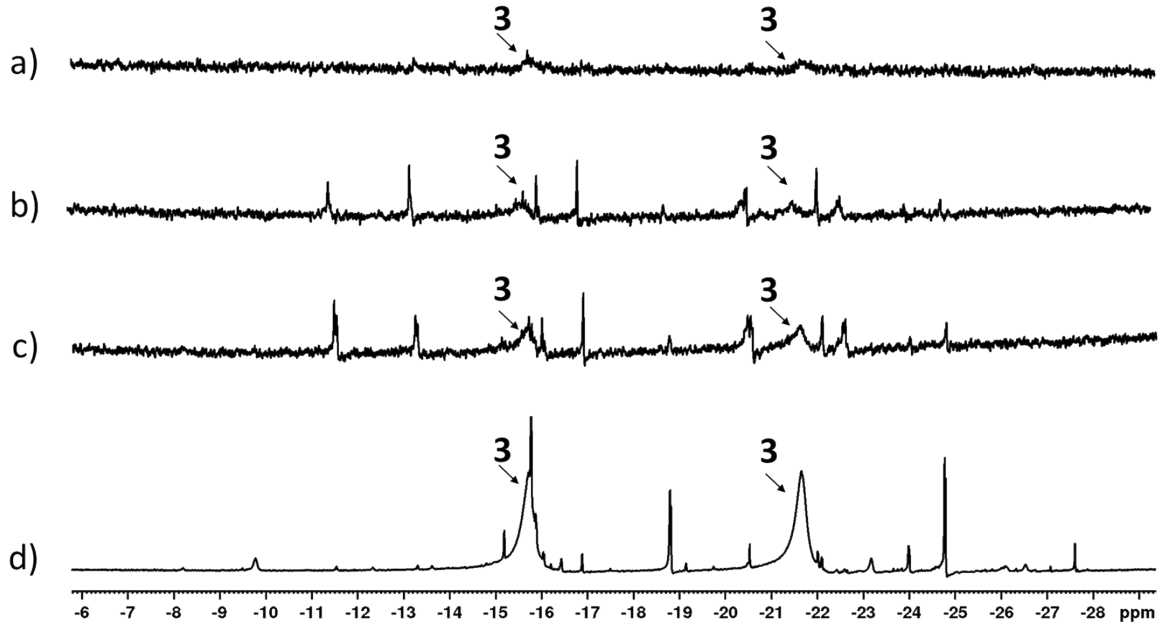

Figure S4: a) ^{1}H NMR spectrum of 3 at 298 K yields broad resonances for the rapidly exchange hydrides b) ^{1}H NMR spectrum of 3 after exposing to oxygen c) ^{1}H NMR spectrum of 3 after isolating as a solid and redissolving in methanol-d_4 d) Synthesis and isolation of a larger batch of 3 (10 mg) yielded a less pure sample. Vertical expansion of a)-c) is not the same as d).

S4. Hyperpolarized NMR spectra of 3

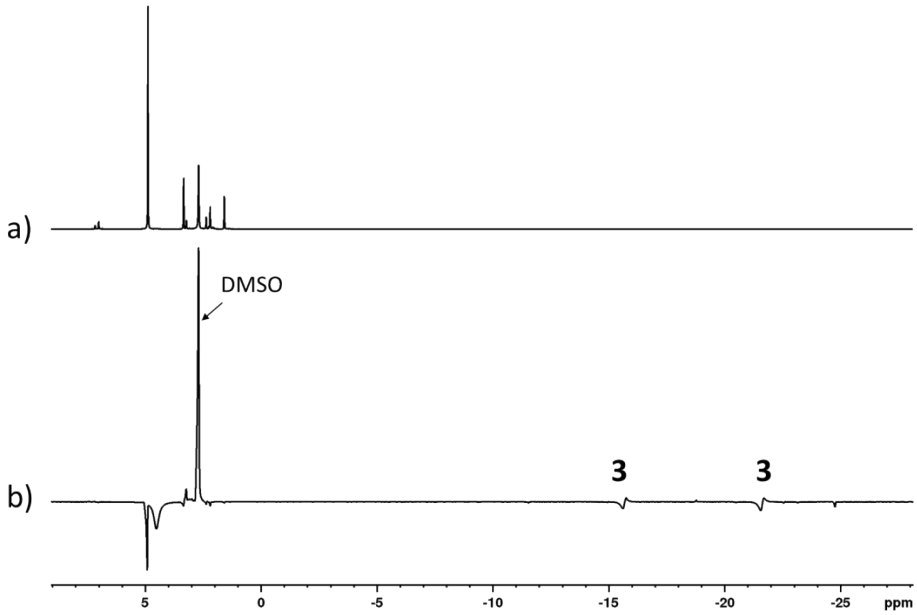

Figure S5: a) ^{1}H Thermal NMR spectrum of 3 at 298 K b) ^{1}H NMR spectrum after shaking 3 with 3-bar *p*-H_2 for 10 seconds at 65 G.

S5. Ligand exchange rates of 3

At low temperatures (245 K) broad hydride resonances of **3** sharpen into resonances corresponding to **3** and **3-*d***.

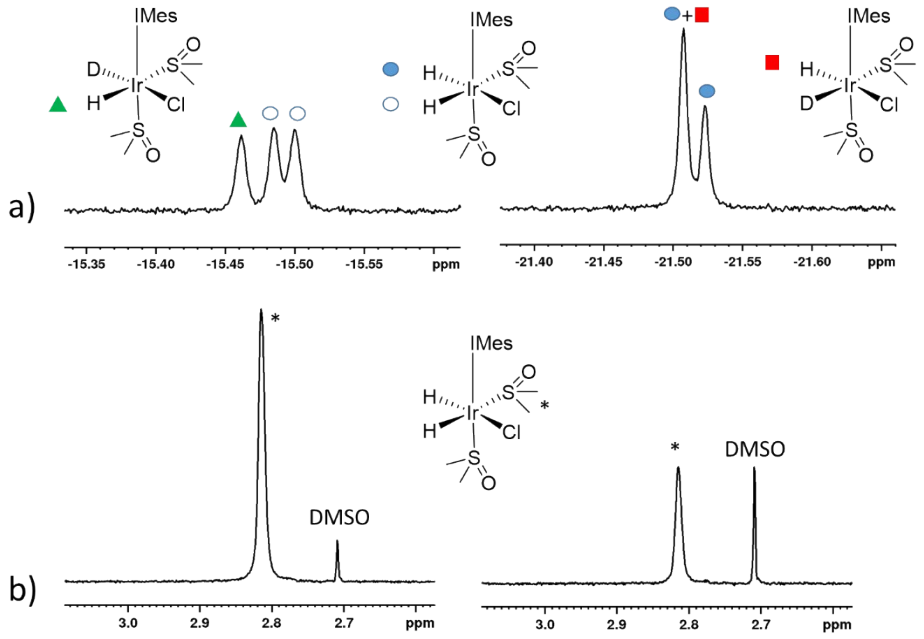

Figure S6: a) ^{1}H NMR spectrum of 3 at 245 K allows distinct resonances for 3 and 3-*d* to be discerned. b) After selective excitation of the bound DMSO resonance *trans* to hydride in 3, exchange to free DMSO is observed after a mixing time of 0.1 s (left). When the mixing time is increased to 0.4 s (right) the free DMSO peak increases in intensity.

Hydrogen exchange (k_{H2}) was measured using Exchange Spectroscopy (EXSY) according to literature procedures.[22] DMSO exchange (k_{DMSO}) was determined in a similar way. The bound DMSO resonance was selectively excited and after set time delays this resonance decreases in intensity and evolves into resonances for free DMSO. The integrals from the NMR spectra at various time delays are interpreted as percentage abundance of bound and free DMSO. A two site exchange model using equations 1-2 has been used to calculate

expected percentage abundances of these bound and free species at varying time delays where $[DMSO]$ and $[3]$ are the concentrations of free DMSO and bound DMSO species respectively, k_{DMSO} and k_{-DMSO} are the rate of DMSO loss and association respectively and $T_{1\,(DMSO)}$ and $T_{1\,(3)}$ are the longitudinal relaxation rates of free and bound DMSO resonances at the same temperature as the EXSY measurement. These equations include relaxation terms in the rate equations which were necessary due to relaxation effects observed at long mixing times.

$$[DMSO]_t = [DMSO]_{t-\delta t} + \left(k_{DMSO}[3]_t - k_{-DMSO}[DMSO]_t - \frac{[DMSO]_t}{T_{1\,(DMSO)}}\right)\partial t \qquad (1)$$

$$[3]_t = [3]_{t-\delta t} + \left(-k_{DMSO}[3]_t + k_{-DMSO}[DMSO]_t - \frac{[3]_t}{T_{1\,(3)}}\right)\partial t \qquad (2)$$

Rate constants were found that give the lowest sum of the least squared fit between calculated percentage abundances using this model, and experimentally determined percentage abundances from EXSY measurements. These are given in Table S6.

Table S6: Rate constants for H_2 and DMSO exchange in methanol-d_4 and DCM-d_2 recorded at different temperatures.

	Methanol-d_4		Dichloromethane-d_2	
	k_{DMSO} /x 10^{-2} s^{-1}	k_{H2} /x 10^{-2} s^{-1}	k_{DMSO} /x 10^{-2} s^{-1}	k_{H2} /x 10^{-2} s^{-1}
233	3.0 ± 0.3	-	-	-
238	7.0 ± 0.2	5.6 ± 0.7	-	-
243	15.2 ± 0.1	16.2 ± 1.0	6.0 ± 0.1	4.1 ± 0.5
248	31.6 ± 0.2	35.1 ± 0.7	13.0 ± 0.2	-
253	64.1 ± 0.2	67.3 ± 1.0	30.7 ± 0.1	25.7 ± 0.7
258	152.1 ± 0.1	151.3 ± 2.0	63.9 ± 0.8	54.1 ± 1.6
263	335.3 ± 0.1	331.4 ± 25.8	156.3 ± 0.9	116.4 ± 4.2
268	728.5 ± 1.8	503.7 ± 36.8	304.6 ± 0.3	256.7 ± 7.8
273	-	-	613.5 ± 1.0	390.3 ± 3.2

Transition state barriers for H_2 and DMSO exchange are calculated by recording rate constants at multiple temperatures as reported previously.[22] The associated Eyring plots are shown in Figure S7.

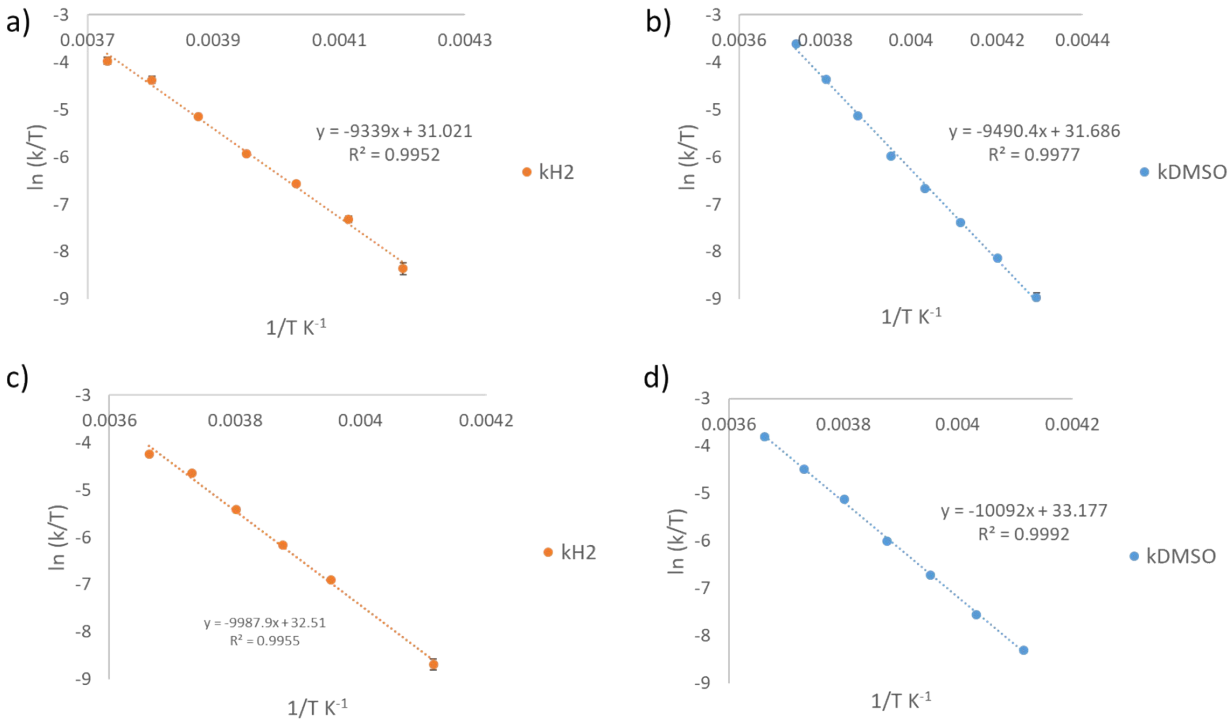

Figure S7: Eyring plots of the data in Table S3 allowing for the transition state barriers of H_2 (a) and c)) and DMSO (b) and d)) exchange in methanol-d_4 (a) and b)) and DCM-d_2 (c) and d)) to be calculated.

In order to prove the reaction proceeds *via* dissociative kinetics, the rate of H_2 loss and DMSO loss where probed as a function of their respective concentrations, as detailed in Figure S8.

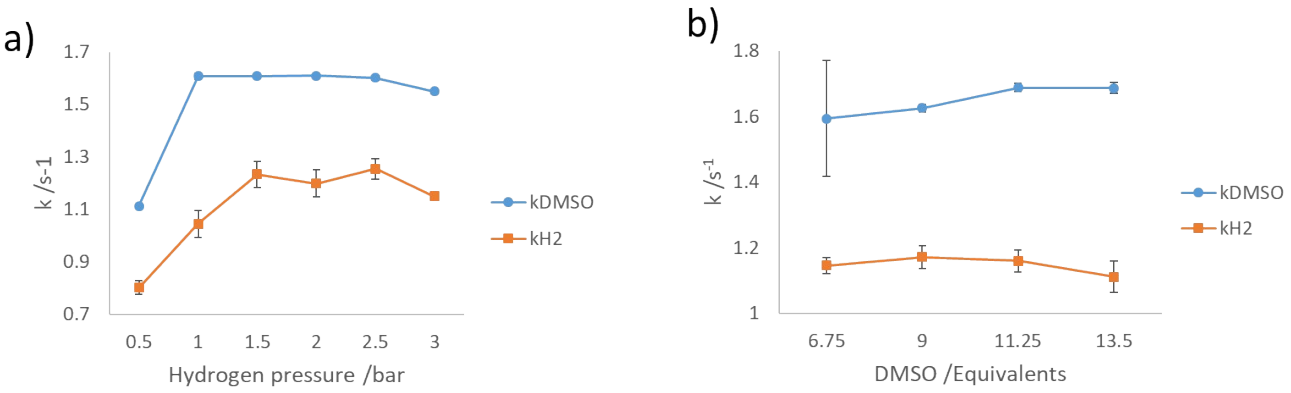

Figure S8: Rates of DMSO and H_2 exchange in a sample of 5 mM 1 in methanol-d_4 at 243 K when the a) H_2 pressure and b) DMSO concentration were varied. In a) the DMSO concentration was fixed at 4.5 equivalents relative to 1 and b) the H_2 pressure was fixed at 3-bar.

S6. References

1. Crystalis-Pro, *Oxford Diffraction Ltd.*, Version 1.171.34.41.
2. O. V. Dolomanov, L. J. Bourhis, R. J. Gildea, J. A. Howard and H. Puschmann, *J. Appl. Cryst.*, 2009, **42**, 339-341.
3. G. Sheldrick, *Acta Crys. Sec. A.*, 2015, **71**, 3-8.
4. G. Sheldrick, *Acta Crys. Sec. C.*, 2015, **71**, 3-8.
5. M. J. Frisch, G. W. Trucks, H. B. Schlegel, G. E. Scuseria, M. A. Robb, J. R. Cheeseman, G. Scalmani, V. Barone, B. Mennucci, G. A. Petersson, H. Nakatsuji, M. Caricato, X. Li, H. P. Hratchian, A. F. Izmaylov, J. Bloino, G. Zheng, J. L. Sonnenberg, M. Hada, M. Ehara, K. Toyota, R. Fukuda, J. Hasegawa, M. Ishida, T. Nakajima, Y. Honda, O. Kitao, H. Nakai, T. Vreven, J. J. A. Montgomery, J. E. Peralta, F. Ogliaro, M. Bearpark, J. J. Heyd, E. Brothers, K. N. Kudin, V. N. Staroverov, T. Keith, R. Kobayashi, J. Normand, K. Raghavachari, A. Rendell, J. C. Burant, S. S. Iyengar, J. Tomasi, M. Cossi, N. Rega, J. M. Millam, M. Klene, J. E. Knox, J. B. Cross, V. Bakken, C. Adamo, J. Jaramillo, R. Gomperts, R. E. Stratmann, O. Yazyev, A. J. Austin, R. Cammi, C. Pomelli, J. W. Ochterski, R. L. Martin, K. Morokuma, V. G. Zakrzewski, G. A. Voth, P. Salvador, J. J. Dannenberg, S. Dapprich, A. D. Daniels, O. Farkas, J. B. Foresman, J. V. Ortiz, J. Cioslowski and D. J. Fox, *Gaussian, Inc., Wallingford CT*, 2010, Gaussian 09, Revision D.01.
6. B. Mennucci, E. Cances and J. Tomasi, *J. Phys. Chem. B*, 1997, **101**, 10506-10517.
7. E. Cances, B. Mennucci and J. Tomasi, *J. Chem. Phys.*, 1997, **107**, 3032-3041.
8. E. Cancès and B. Mennucci, *J. Math. Chem.*, 1998, **23**, 309-326.
9. C. Adamo and V. Barone, *J. Chem Phys.*, 1999, **110**, 6158-6170.
10. F. Weigend and R. Ahlrichs, *Phys. Chem. Chem. Phys.*, 2005, **7**, 3297-3305.
11. A. Schäfer, H. Horn and R. Ahlrichs, *J. Chem. Phys.*, 1992, **97**, 2571-2577.
12. D. Feller, *J. Comput. Chem.*, 1996, **17**, 1571-1586.
13. K. L. Schuchardt, B. T. Didier, T. Elsethagen, L. Sun, V. Gurumoorthi, J. Chase, J. Li and T. L. Windus, *J. Chem. Inf. Model.*, 2007, **47**, 1045-1052.
14. L. E. Roy, P. J. Hay and R. L. Martin, *J. Chem. Theory Comput.*, 2008, **4**, 1029-1031.
15. S. Grimme, S. Ehrlich and L. Goerigk, *J. Comput. Chem.*, 2011, **32**, 1456-1465.
16. C. R. M. Buehl, D. Pantazis, T. Bredow and F. Neese, *J. Chem. Theor. Comput.*, 2008, **4**, 1449-1459.
17. J. E. Richards, A. J. J. Hooper, O. W. Bayfield, M. C. R. Cockett, G. J. Dear, A. J. Holmes, R. O. John, R. E. Mewis, N. Pridmore and A. D. Roberts, *Chem. Commun.*, 2018, **54**, 10375-10378.
18. B. J. Tickner, R. O. John, S. S. Roy, S. Hart, A. C. Whitwood and S. B. Duckett, *Chem Sci*, 2019, **10**, 5235-5245.
19. S. F. Boys and F. Bernardi, *Mol. Phys.*, 1970, **19**, 553.
20. S. Simon, M. Duran and J. J. Dannenberg, *J. Chem. Phys.*, 1996, **105**, 11024-11031.
21. W. Iali, S. S. Roy, B. J. Tickner, F. Ahwal, A. J. Kennerley and S. B. Duckett, *Angew. Chem.*, 2019, DOI: 10.1002/ange.201905483.
22. B. J. Tickner, W. Iali, S. S. Roy, A. C. Whitwood and S. B. Duckett, *ChemPhysChem*, 2019, **20**, 241-245.